J. Cell. Mol. Med. Vol 16, No 3, 2012 pp. 468-482

Cardiomyocytes generated from CPVT^{D307H} patients are arrhythmogenic in response to β-adrenergic stimulation

Atara Novak [a, b, c], Lili Barad [a, b, c], Naama Zeevi-Levin [a, c], Revital Shick [a, b, c], Ronit Shtrichman [a, c], Avraham Lorber [c, d], Joseph Itskovitz-Eldor [a, c, e, *], Ofer Binah [a, b, c, *]

[a] *The Sohnis Family Stem Cells Center, Haifa, Israel*
[b] *The Rappaport Family Institute for Research in the Medical Sciences, Haifa, Israel*
[c] *Ruth & Bruce Rappaport Faculty of Medicine, Technion – Israel Institute of Technology, Haifa, Israel*
[d] *Department of Pediatric Cardiology, Rambam Health Care Campus, Haifa, Israel*
[e] *Department of Obstetrics and Gynecology, Rambam Health Care Campus, Haifa, Israel*

Received: October 21, 2011; Accepted: October 26, 2011

Abstract

Sudden cardiac death caused by ventricular arrhythmias is a disastrous event, especially when it occurs in young individuals. Among the five major arrhythmogenic disorders occurring in the absence of a structural heart disease is catecholaminergic polymorphic ventricular tachycardia (CPVT), which is a highly lethal form of inherited arrhythmias. Our study focuses on the autosomal recessive form of the disease caused by the missense mutation D307H in the cardiac calsequestrin gene, CASQ2. Because CASQ2 is a key player in excitation contraction coupling, the derangements in intracellular Ca^{2+} handling may cause delayed afterdepolarizations (DADs), which constitute the mechanism underlying CPVT. To investigate catecholamine-induced arrhythmias in the CASQ2 mutated cells, we generated for the first time CPVT-derived induced pluripotent stem cells (iPSCs) by reprogramming fibroblasts from skin biopsies of two patients, and demonstrated that the iPSCs carry the CASQ2 mutation. Next, iPSCs were differentiated to cardiomyocytes (iPSCs-CMs), which expressed the mutant CASQ2 protein. The major findings were that the β-adrenergic agonist isoproterenol caused in CPVT iPSCs-CMs (but not in the control cardiomyocytes) DADs, oscillatory arrhythmic prepotentials, after-contractions and diastolic $[Ca^{2+}]_i$ rise. Electron microscopy analysis revealed that compared with control iPSCs-CMs, CPVT iPSCs-CMs displayed a more immature phenotype with less organized myofibrils, enlarged sarcoplasmic reticulum cisternae and reduced number of caveolae. In summary, our results demonstrate that the patient-specific mutated cardiomyocytes can be used to study the electrophysiological mechanisms underlying CPVT.

Keywords: catecholaminergic polymorphic ventricular tachycardia (CPVT) • induced pluripotent stem cells (iPSCs) • arrhythmias • cardiomyocytes • calcium transients and contractions • delayed afterdepolarizations (DADs) • oscillatory prepotentials

Introduction

Catecholaminergic polymorphic ventricular tachycardia (CPVT) is a highly lethal form of inherited arrhythmogenic disease characterized by catecholamines-mediated polymorphic ventricular tachycardia, which can cause sudden death. In 2001 Priori *et al.* [1] identified mutations in the cardiac ryanodine receptor (RyR2) underlying an autosomal dominant form of CPVT. Following Priori's discovery of the pathologic mutations in four CPVT probands [1], a major advancement in understanding CPVT was

*Correspondence to: Ofer BINAH,
Department of Physiology,
Bruce Rappaport Faculty of Medicine,
POB 9649, Haifa 31096, Israel.
Tel.: +972-4-8295262
Fax: +972-4-8513919
E-mail: binah@tx.technion.ac.il

Joseph ITSKOVITZ-ELDOR,
Department of Obstetrics and Gynecology,
Rambam Health Care Campus and Ruth & Bruce Rappaport Faculty of Medicine, POB 9649, Haifa 31096, Israel.
Tel.: +972-4-8542536
Fax: +972-4-8542503
E-mail: itskovitz@rambam.health.gov.il

doi:10.1111/j.1582-4934.2011.01476.x

achieved when an autosomal recessive form of the disease encoding for the calsequestrin (CASQ2) gene was identified in a Bedouin tribe residing in the Northern part of Israel [2]. Direct sequencing of the CASQ2 exons in the Bedouin patients revealed a *G* to *C* nonsynonymous substitution at nucleotide 1183, converting an aspartic acid to histidine at position 307 (D307H) of the protein. CASQ2 is a high-capacity, low affinity Ca^{2+} binding protein, operating as a major Ca^{2+} buffering factor. Because this protein is a key player in the excitation contraction coupling process, the functional derangements in intracellular Ca^{2+} handling resulting from the mutated CASQ2 gene may cause delayed after-depolarizations (DADs) which constitute the major electrophysiological mechanism underlying CPVT [3]. Despite the paramount advancement in understanding the diverse aspects of CPVT, this fatal disease still presents high mortality rates among young as well as older individuals. Further, although the electrophysiological basis of CPVT was investigated in several *in vitro* and *in vivo* models [3–8], the mechanisms underlying the arrhythmogenesis are not entirely understood. In order to investigate directly cardiomyocytes expressing the mutated CASQ2 gene, we generated patient-specific induced pluripotent stem cells (iPSCs) from dermal fibroblasts obtained from two members of a family affected by CPVT, from the Bedouin tribe carrying the missense mutation D307H. Recently several groups reported on the generation of patient-specific iPSCs from patients affected by long-QT syndrome type 1 [9], long-QT syndrome type 2 [10] and Timothy syndrome [11], and showed the capacity of these cells to give rise to functional cardiomyocytes that display the electrophysiological characteristics of the disorder. To this end we report here for the first time on the generation of functional CPVT iPSCs-derived cardiomyocytes (CPVT iPSCs-CMs), which in response to the β-adrenergic agonist isoproterenol generated DADs and oscillatory prepotentials, as well as after-contractions and diastolic $[Ca^{2+}]_i$ rise. Collectively these findings demonstrate the arrhythmic features of the disease. This technology will provide us the means to advance our understanding of CPVT, and hopefully to improve its future clinical outcome.

Materials and methods

Generation of patient-specific iPSCs

Skin biopsies and hair were acquired according to approval #3611 issued by the Helsinki Committee for experiments on human subjects at the Rambam Health Care Campus, Haifa, Israel. Skin biopsies [human dermal fibroblasts (HDF)] were obtained from two CPVT patients; a 12-year-old boy (HDF7) and a 30-year-old woman (HDF12) from the affected Bedouin tribe, and from two healthy controls; a 25-year-old male (HDF5) and a 23-year-old female (HDF3). Hair keratinocytes were obtained from one healthy control, a 42-year-old female (KTR). iPSCs were generated from human dermal fibroblasts (CPVT clones 7.5, 7.6, 12.4, and control clones 3.3 and 5.2, from biopsies HDF7, HDF12, HDF3 and HDF5, respectively) and hair keratinocytes (clone KTR13 from the KTR biopsy) [12], using the STEMCCA Cassette (a single lentiviral vector containing the four factors: oct4, sox2, klf4 and c-myc) as previously described [12–14].

Genotyping

Genomic DNA was purified using the Promega (Madison, WI, USA) DNA purification kit. PCR was performed to the CASQ2 gene using the primers: F-5'-CACTCTGCTCTCCACATTAGAAGCTGT-3' and R-5'-AAAAG-TAGTTCTGGGGACTGGGAATGG-3' resulting in a product length of 495 nucleotides.

Karyotype analysis

Karyotype analysis was performed using standard G-banding chromosome analysis by the cytogenetic laboratory according to standard procedures.

RNA analysis

RNA was isolated from 28- to 30-day-old EBs using AurumTM Total RNA Mini Kit (BIO-RAD, Hercules, CA, USA) and reverse transcribed by the iScriptTM cDNA synthesis kit (BIO-RAD), according to the manufacturer's instructions. PCR was performed by DreamTaqTM Green Master Mix (Fermentas, Ontario, Canada). The primers used for RNA analysis are listed in Table 1.

Immunofluorescence

Immunofluorescence staining was performed according to standard protocols using the following antibodies: rabbit anti-Oct3/4 (1:100; Santa Cruz, CA, USA), goat anti-nanog (1:20; R&D, Minneapolis, MN, USA), mouse anti-Sox2 (1:100; Millipore, Santa Cruz, CA, USA), mouse anti-TRA 1–60 (1:100; Millipore), mouse anti-TRA 1–81 (1:100; Millipore), mouse anti-SSEA4 (1:100; Hybridoma Bank, Iowa city, IA, USA), mouse anti-Nestin (1:100; Chemicon, Temecula, CA, USA), rabbit anti-tubulin IIIβ (1:2000; Covance, Princeton, NJ, USA), rabbit anti-glial fibrillary acidic protein GFAP (1:200; Millipore), mouse anti-CD31 (1:100; AnCell, Bayport, MN, USA), rabbit anti-von Willebrand factor vWF (1:100; Dako, Glostrup, Denmark), mouse anti-smooth muscle actin SMA (1:100; Dako), rabbit anti-alpha fetoprotein AFP (1:1; Dako), mouse anti-glucagone (1:50; Dako), rabbit anti-cardiac troponin I (1:400; Abcam, Cambridge, UK), mouse anti-sarcomeric α-actinin (1:600; Sigma-Aldrich, St. Louis, MO, USA), mouse anti-α/β myosin heavy chain (1:40; Chemicon), rabbit anti-cardiac calsequestrin CASQ2 (1:100; Santa Cruz) and goat anti-triadin (1:100; Santa Cruz). Secondary antibodies were as follows: donkey anti-rabbit Cye 3 (1:100; Chemicon) and donkey anti-mouse/goat Alexafluor 488 (1:100; Invitrogen, Carlsbad, CA, USA). Cells were also stained with DAPI (1:1000; Boehringer, Mannheim, Germany) for nuclei detection.

Measurements of intracellular Ca^{2+} transients and contractions

Intracellular Ca^{2+} ($[Ca^{2+}]_i$) transients and contractions were measured from small contracting areas of EBs (25–43-day-old EBs) by means of fura-2 fluorescence and video edge detector, respectively as previously described [15, 16]. Induced pluripotent stem cells were spontaneously differentiated toward cardiomyocytes [16, 17], and spontaneously contracting areas from

Table 1 Primers used for RT-PCR

Gene	Sequence (5′ to 3′)	Product size (bp)
Cardiac Troponin-T	F- GGCAGCGGAAGAGGATGCTGAA	152
	R- GAGGCACCAAGTTGGGCATGAACGA	
Calsequestrin 2 (CASQ2)	F- GTATATTCTTAAGGGTGATCGCACA	314
	R- GCTCATAGAAGTCAACCTCATTCAT	
Calreticulin	F- GAGAAAGATAAAGGTTTGCAGACAA	339
	R- TGTGTACAGGTGTGTAAACTCATCA	
Triadin	F- TTACAAAAACTTTTCAGCAAGCTCT	434
	R- TTTCTTCACTCTTTTCTGCAGTCTT	
Junctin	F- AAAGCATGGAGGACACAAGAAT	174
	R- AAGTTATAACGGAAGTCCTTTGCTT	
SERCA2	F- ACAGAGTGGAAGGTGATACTTGTTC	384
	R- AGTAAACCGACATTGACTTTCTGTC	
NCX1	F- AAGTGACTGAAAATGACCCTGTTAG	401
	R- AAAAATAGTTACAGTGGCAGTGGAG	
Ryanodine receptor 2 (RyR2)	F- ATCCACAAAGAACAACAGAAGCTAT	509
	R- CCATAAGACAAGTGCAAGTACCTTT	
GAPDH	F-GCCTGCTTCACCACCTTC	100
	R-AATCCCATCACCATCTTC	

2–3-week-old EBs were mechanically dissected, and adhered onto gelatin coated glass slides. Subsequently, fura 2-stained contracting areas were transferred to a chamber mounted on the stage of an inverted microscope, and perfused at a rate of 1–1.5 ml/min. at 37°C, with Tyrode's solution containing (mmol/l); 140 NaCl, 5.4 KCl, 1 $MgCl_2$, 2 sodium pyrovate, 1 $CaCl_2$, 10 HEPES, 10 glucose (pH 7.4 with NaOH). The preparations were stimulated at a frequency 10% higher than the spontaneous rate; in the majority of experiments a stimulation frequency of 0.5–1 Hz was sufficient to override the spontaneous beating rate. The acquisition rate of both the $[Ca^{2+}]_i$ transients and contractions was 100 points/sec. To characterize the contraction amplitude, the differences between minimal and maximal video cursor positions (L_{Amp}) were calculated in 10 successive contractions and averaged. In addition, the maximal rates of contraction ($dL/dt_{Contraction}$) and relaxation ($dL/dt_{Relaxation}$) were calculated and averaged over 10 contractions.

Measurements of transmembrane action potentials

Action potentials were recorded from spontaneously contracting small cell clusters or isolated cells generated by dissociating control and CPVT iPSCs-CMs, following plating on top of gelatin or fibronectin-coated glass coverslips. The patch pipette solution contained (mM): 120 KCl, 1 $MgCl_2$, 3 Mg-ATP, 10 HEPES, 10 EGTA (pH7.3). The bath solution contained (mM): 140 NaCl, 5.4 KCl, 1.8 $CaCl_2$, 1 $MgCl_2$, 10 HEPES, 10 glucose (pH7.4) (all materials were purchased from Sigma-Aldrich). Axopatch 200B, Digidata 1322 and pClamp10 (Molecular Devices, Sunnyvale, CA, USA) were used for data amplification, acquisition and analysis.

Transmission electron microscopy

Transmission electron microscopy (TEM) was performed on 31-day-old (post-plating) iPSCs-EBs from a CPVT patient (n = 3) and from healthy controls (n = 3) fixed with 2.5% glutaraldehyde in 0.1 M cacodylate buffer. The samples were further processed for epoxy resin (Agar100) embedded as previously reported [18]. TEM was performed using a Morgagni 286 transmission electron microscope (FEI Company, Eindhoven, The Netherlands) at 80 kV. Digital electron micrographs were recorded with a MegaView III CCD and iTEM-SIS software (Olympus, Soft Imaging System GmbH, Münster, Germany).

Statistical analysis

The results are presented as mean ± S.E.M. Paired or unpaired *t*-test was performed to compare between the means of two populations. $P < 0.05$ was considered statistically significant.

Results

Molecular characterization of CPVT-derived iPSCs

The iPSCs derived from CPVT patients and healthy controls were maintained for up to 60 passages thus far, and had human embryonic stem cell (hESC)-like morphology (Fig. 1A), as well as normal and stable karyotype (Fig. 1B). Next, as seen in Figure 1C, the CPVT iPSCs and the control clones (data not shown for HDF; see ref [12] for keratinocytes) were characterized, and were found to express the typical pluripotent markers Oct4, Sox2, Nanog, SSEA4, TRA1-60 and TRA1-81, as demonstrated by immunostaining. Pluripotency was confirmed by the spontaneous differentiation into derivatives of all three germ layers, by the means of the *in vitro* test through EBs formation (Fig. 1D) and *in vivo* using the teratoma assay (Fig. 1E).

Genotyping the CPVT mutation

In order to confirm that the mutation is preserved in the iPSCs clones, we performed PCR reaction to genomic DNA with primers that delimit the mutation area on the CASQ2 gene. As described by Lahat and co-workers [2], the missense mutation in the CASQ2 gene causes the substitution of *G* to *C* at nucleotide 1183, and creates a BamHI restriction site in the mutated sequence. As demonstrated in Figure 2A, the fibroblasts HDF7 originating from the CPVT patient carry the missense mutation in both copies of the chromosomes. The iPSCs clones 7.5 and 7.6 derived from the CPVT fibroblasts preserved the $CASQ2^{D307H}$ mutation whereas none of the control fibroblasts (HDF3, HDF5) or the control iPSCs clones (5.2 and 3.3) exhibited the mutation. Additionally, we performed full sequencing of the genomic PCR product, and confirmed the switch of *G* to *C* at nucleotide 1183 in the CASQ2 gene (Fig. 2B).

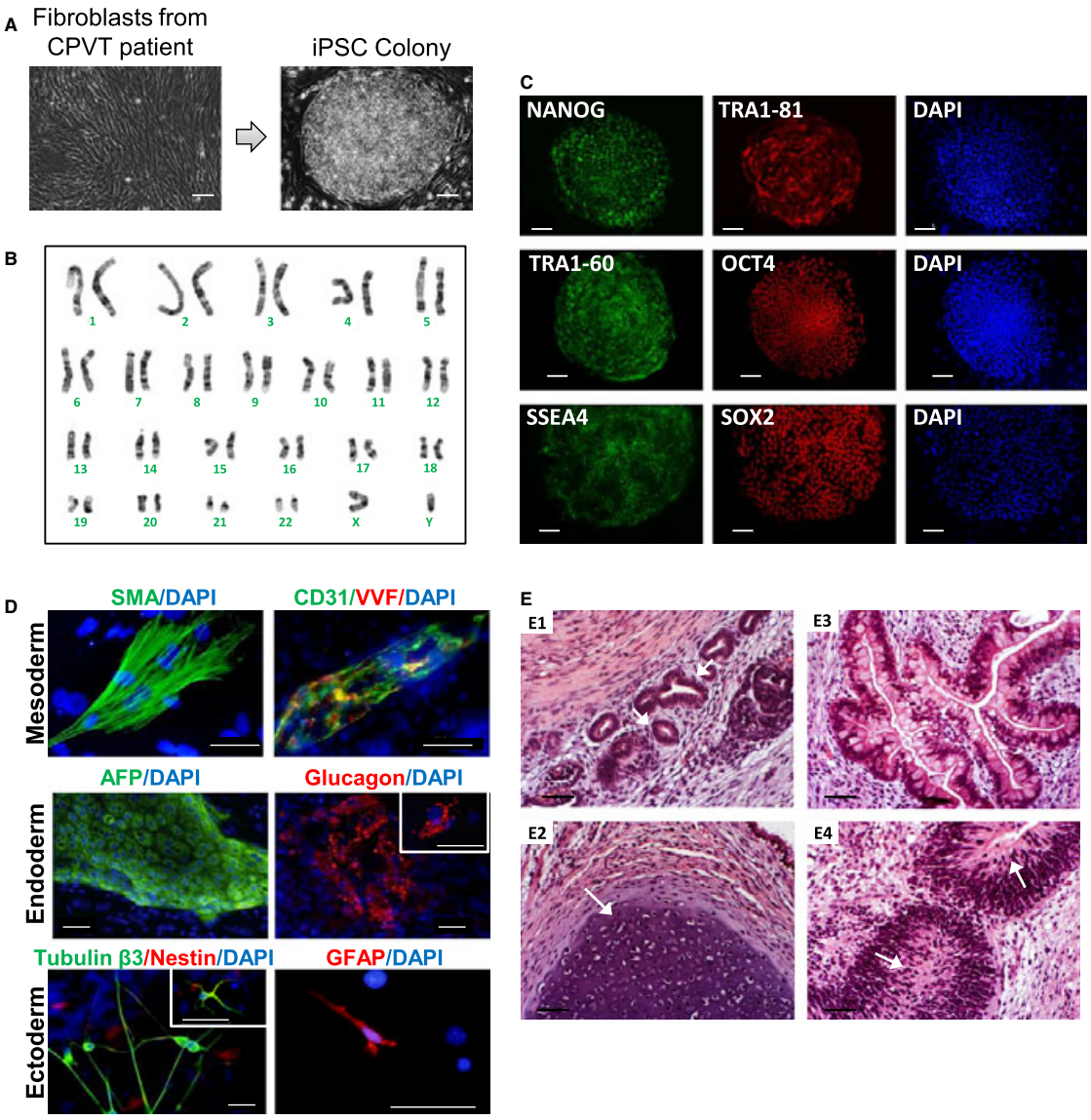

Fig. 1 Generation of pluripotent stem cells from healthy and CPVT patients. (**A**) Primary skin fibroblasts derived from a CPVT patient skin biopsy, and a corresponding representative iPSC colony. (**B**) Karyotype analysis of iPSCs from a CPVT patient. (**C**) Immunostaining of typical pluripotent markers shown for the iPSCs derived from the CPVT patient, clone HDF7.5. Nuclei were stained with DAPI (blue). Scale bar: 100 μm. (**D**) Immunostaining of 21-day-old EBs derived from the iPSCs-HDF7.5 demonstrates expression of mesodermal (SMA, CD31, vWF), endodermal (AFP, glucagon) and ectodermal (tubulin-β3, nestin, GFAP) marker proteins. Nuclei were stained with DAPI (blue). Scale bar: 50 μm. (**E**) Histological analysis of a representative teratoma obtained from *in vivo* differentiated cells of iPSCs-HDF7.6. The formed teratomas contained derivatives of all three germ layers (ectoderm, mesoderm and endoderm). (**E1**) Muscle (left-up of image, mesoderm) and endocrine glands (arrow, endoderm). (**E2**) Cartilage (arrow, mesoderm). (**E3**) Gut epithelium (endoderm). (**E4**) Neural-like tissues at arrow (ectoderm). All images were obtained from formalin-fixed and paraffin-embedded teratoma sections stained with haematoxylin and eosin. Scale bar: 50 μm.

Differentiation of CPVT iPSCs into functional cardiomyocytes

Next, the control and CPVT iPSCs were spontaneously differentiated into functional cardiomyocytes as previously described [16, 17]. Immunofluorescence staining of micro-dissected contracting areas (Fig. 3A) demonstrated that the cardiomyocytes co-express the typical cardiac markers, cardiac troponin I and α-sarcomeric actinin. Importantly, the cardiomyocytes exhibited areas of cross-striations, indicating organization toward myofibrilar structures.

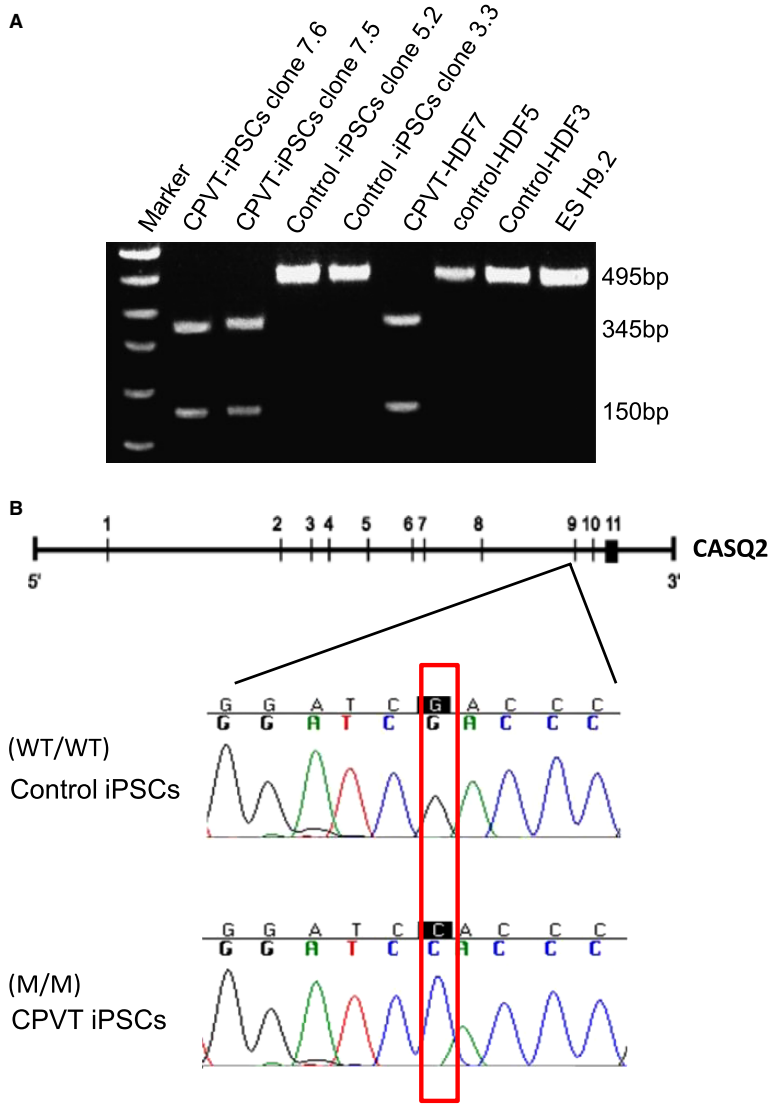

Fig. 2 Characterization of the calsequestrin D307H mutation. (**A**) BamHI restriction analysis of the D307H mutation for the control and CPVT iPSCs clones, and their parental cells (HDF). Human embryonic stem cells (clone H9.2) are included for comparison. The substitution at nucleotide 1183 creates a BamHI restriction site in the mutated sequence. The 495bp PCR product of genomic DNA is cleaved in the CPVT patient chromosome to 150bp and 345bp products. (**B**) Sequence analysis of genomic CASQ2 obtained from iPSCs derived from control subject (WT/WT) and CPVT patient (M/M) revealing a homozygous missense mutation in CASQ2 exon 9, in position 569 of the coding sequence, converting aspartic acid to histidine at position 307 of the protein.

Next, PCR analysis was performed in order to determine whether key genes involved in the Ca^{2+} handling process or interact with CASQ2, are expressed in CPVT cardiomyocytes. The PCR analysis (Fig. 3B) shows the expression of CASQ2, calreticulin, junctin, triadin, NCX1, SERCA2 and RyR2 in control and CPVT iPSCs-EBs, and in EBs from clone H9.2 of hESC. These findings were repeated in three experiments.

To ascertain that the mutant cardiomyocytes express both the CASQ2 (albeit the mutated form $CASQ2^{D307H}$) and triadin proteins (the latter being sarcoplasmic reticulum (SR) membrane protein interacting with CASQ2), co-immunofluorescence staining with α-sarcomeric actinin was performed. As seen in Figure 4A, the double staining of α-sarcomeric actinin with CASQ2 shows that the small clusters of EBs composed of cardiomyocytes express the cardiac CASQ2, in contrast to H9.2-CMs which were previously reported not to express the protein [16, 19, 20]. Further, as seen in Figure 4B, in both control and CPVT cardiomyocytes, the CASQ2 signal was co-localized with triadin, an observation consistent with the fact that both proteins interact at the RyR2 complex. Finally, as seen in Figure 3C, the beating rate was measured in spontaneously contracting EBs, and was found to be 25.7 ± 1.5 ($n = 20$) in CPVT iPSCs-CMs and 38.8 ± 3.6 bpm (beats per minute) in control iPSCs-CMs ($n = 10$), $P < 0.01$.

Transmission electron microscopy (TEM) analysis of control and CPVT iPSCs-CMs

In order to evaluate the ultrastructural characteristics of CPVT iPSCs-CMs, we performed a comparative TEM analysis with

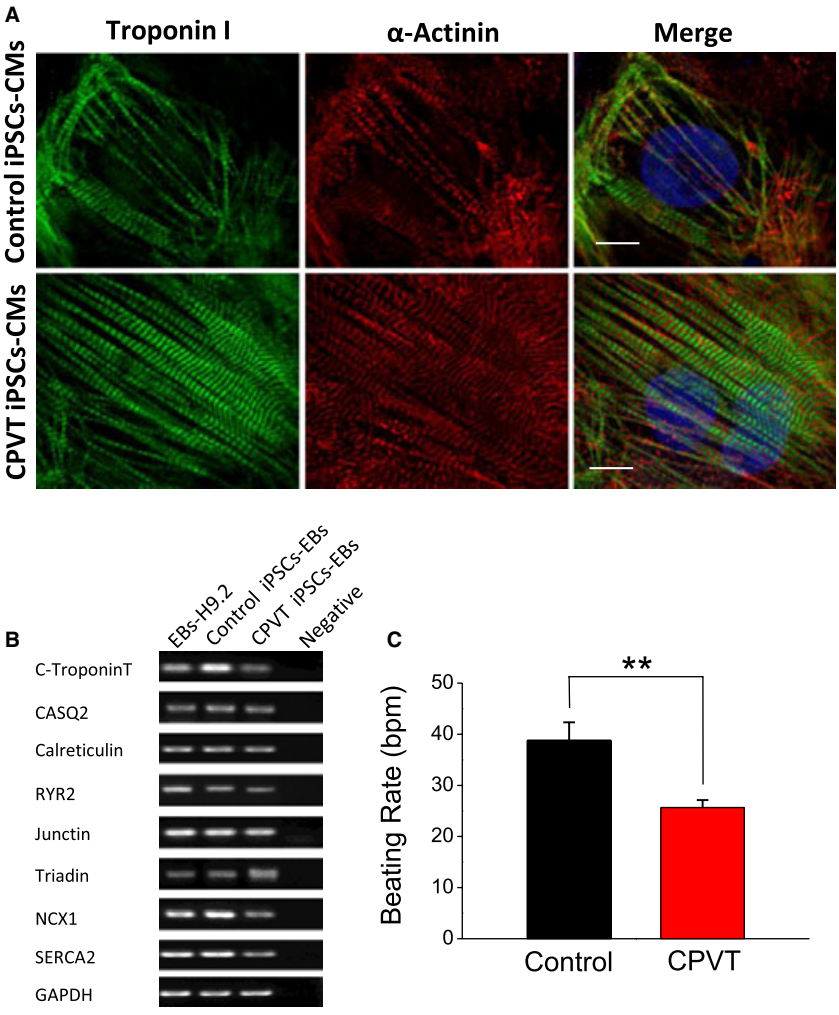

Fig. 3 Characterization of CPVT iPSCs-CMs. (**A**) Micro-dissected contracting areas from the control and CPVT iPSCs-CMs were stained for typical myofilament proteins. The cardiomyocytes were co-labelled with anti-cardiac troponin I (green) and anti-sarcomeric α-actinin (red). (**B**) Representative PCR analysis of the cardiac gene troponin-T, and the calcium associated genes CASQ2, calreticulin, RyR2, junctin, triadin, NCX1, SERCA2 and the housekeeping gene GAPDH (n = 2). (**C**) The spontaneous beating rate of control iPSCs-CMs (n = 10) and CPVT iPSCs-CMs (n = 20). bpm: beats per minute. $^{**}P < 0.01$. Scale bar: 10 μm.

control iPSCs-CMs (Fig. 5). The analysis demonstrated that the control (Fig. 5A) and CPVT iPSCs (Fig. 5B) differentiated into cardiomyocytes with immature ultrastructural features. Cardiomyocytes in both groups (Fig. 5A and B) had large glycogen deposits, lipid droplets, mitochondria, free ribosomes, rough endoplasmic reticulum and SR. T-tubules were not found in either control or CPVT iPSCs-CMs. Additionally, the organization of myofibrils appeared to be more mature in control iPSCs-CMs (Fig. 5C) than in CPVT iPSCs-CMs (Fig. 5D). The myofibrils in the control group were approximately 1.5 μm wide and were formed by up to eight consecutive sarcomeres [18]. In contrast, the myofibrils in CPVT iPSCs-CMs were narrower, about 0.5 μm (0.58 ± 0.26) and were formed by up to 5 consecutive sarcomeres. Further, SR and 'Ca^{2+}-release units' connecting the peripheral SR with the plasmalemma were present in both control (Fig. 5E) and CPVT iPSCs-CMs (Fig. 5F). In addition, small SR cisternae were present in the vicinity of the Z bands (Fig. 5F). CPVT iPSCs-CMs displayed small areas with abnormal dilated or fragmented SR cisternae (Fig. 5G), and the average width of peripheral SR was wider (22.67 ± 8.99 nm) than the control value (16.12 ± 4.02 nm). Finally, CPVT iPSCs-CMs had a considerably reduced number of caveolae (0.01 caveolae/μm) compared with control (0.35 caveolae/μm). The number of caveolae was counted along a 100 μm length of plasmalemma in 20 randomly selected cells for each group.

β-adrenergic stimulation caused arrhythmias and diastolic $[Ca^{2+}]_i$ rises in CPVT iPSCs-CMs

The adrenergically mediated arrhythmogenic features of CPVT iPSCs-CMs were demonstrated by exposing cardiomyocytes to isoproterenol. As depicted in Figure 6A–C, while in control cardiomyocytes isoproterenol increased contraction amplitude

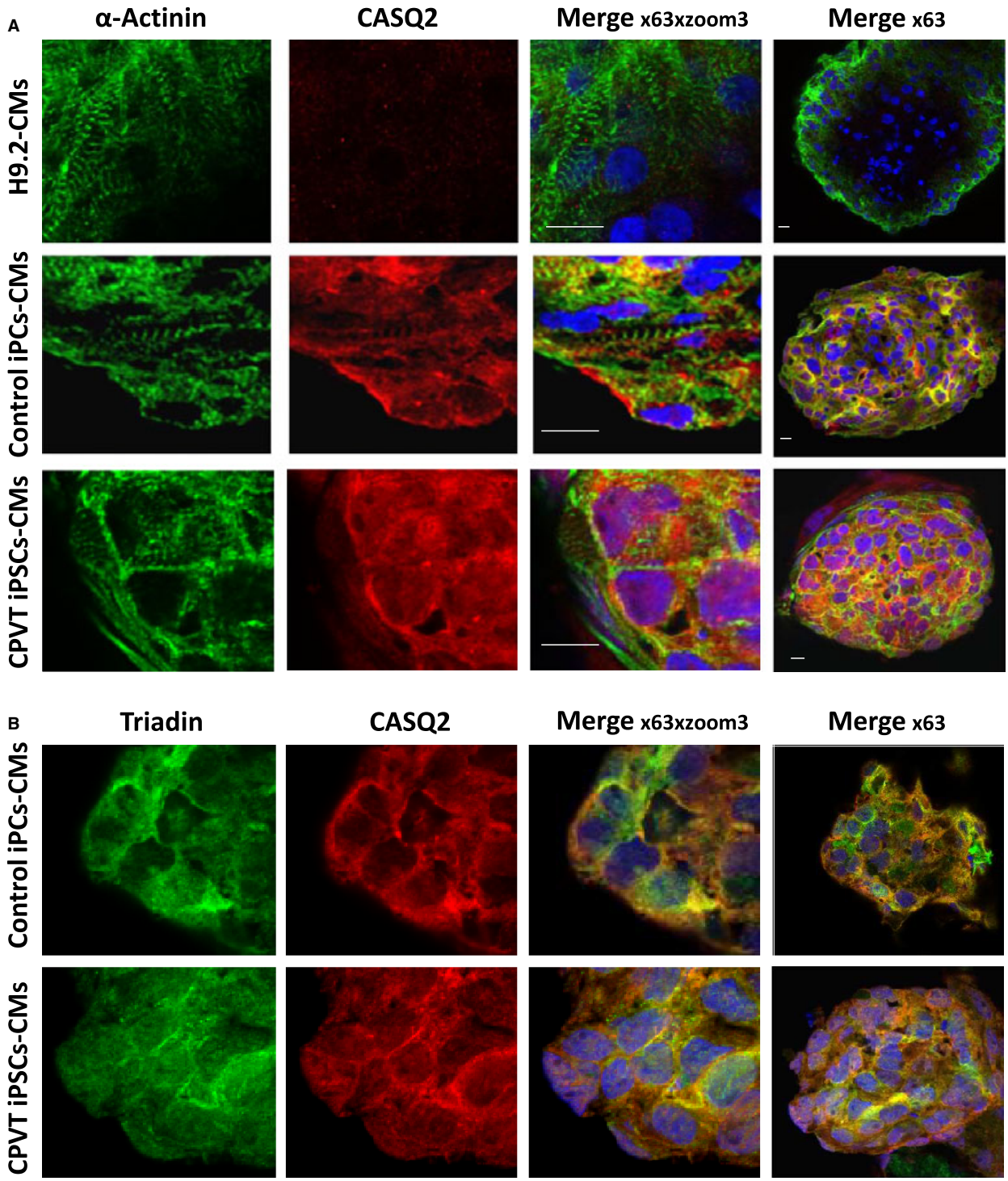

Fig. 4 CASQ2 and triadin immunofluorescence expression in control and CPVT iPSCs- derived cardiomyocytes. Micro-dissected contracting areas from H9.2-CMs and from the control and CPVT iPSCs-CMs stained for (**A**) anti-cardiac calsequestrin (CASQ2, red) with anti-sarcomeric α-actinin (green), and (**B**) anti-cardiac calsequestrin (CASQ2, red) with anti-triadin (green). Nuclei were stained with DAPI (blue). Scale bar: 10 μm.

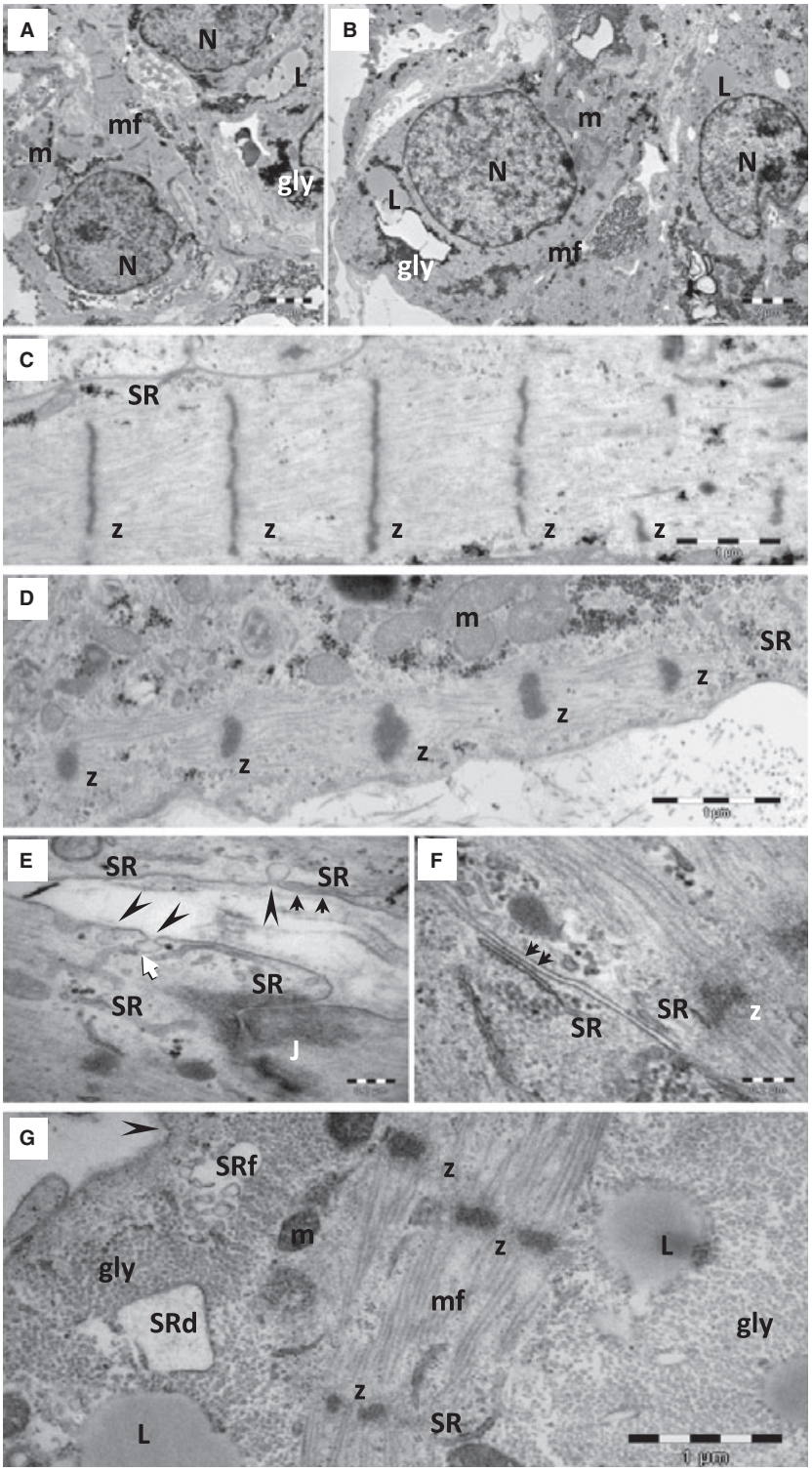

Fig. 5 Transmission electron microscopy (TEM) analysis in control iPSCs-CMs (**A, C, E**) and CPVT iPSCs-CMs (**B, D, F, G**). (**A**) TEM of control iPSCs-CMs and (**B**) CPVT iPSCs-CMs shows cells with myofibrils (mf), glycogen (gly), mitochondria (m) and lipid droplets (L). N: nucleus. (**C**) Note large sarcomeres in control iPSCs-CMs, and (**D**) slender sarcomeres in CPVT iPSCs-CMs. Z: Z bands; SR: sarcoplasmic reticulum. (**E–F**) Ultrastructure of 'Ca^{2+}-release units' (small arrows) formed by ryanodine receptors between peripheral SR and plasmalemma in control iPSCs-CMs (**E**) and CPVT iPSCs-CMs (**F**). Note the connection (white arrow) between caveolae (arrowheads) and SR in Control iPSCs-CMs. J: junction. (**G**) A CPVT-iPSCs-cardiomyocyte with normal SR, and SR with dilated (SRd) and fragmented (SRf) cisternae. Z: Z bands; gly: glycogen; L: lipid droplets; mf: myofilaments.

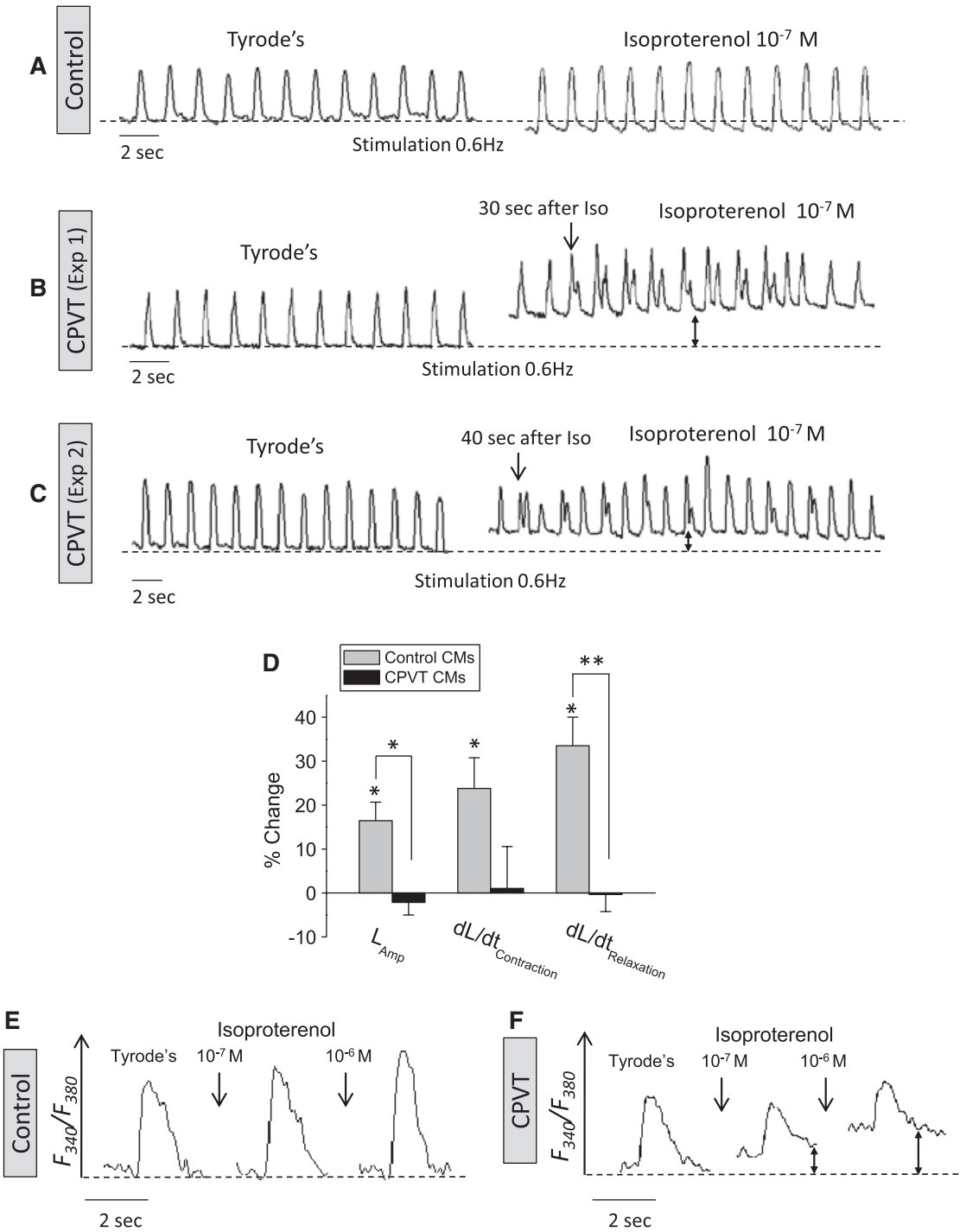

Fig. 6 The effects of isoproterenol on the $[Ca^{2+}]i$ transients and contractions in control and CPVT iPSCs-CMs. (**A**) Representative contractions tracings of control iPSCs-CMs (43-day-old EB) stimulated at 0.6 Hz, in the absence (Tyrode's) and presence of isoproterenol. (**B**–**C**) Representative contractions tracings of CPVT iPSCs-CMs (33- and 38-day-old EBs, respectively) stimulated at 0.6 Hz, in the absence (Tyrode's) and the presence of isoproterenol. Note that after-contractions developed only in the CPVT cardiomyocytes in the presence of isoproterenol. (**D**) The effects of isoproterenol on contraction parameters of control iPSCs-CMs and CPVT iPSCs-CMs, $*P < 0.05$. (**E**–**F**) Representative $[Ca^{2+}]i$ transients of control iPSCs-CMs (40-day-old EB) and CPVT iPSCs-CMs (34-day-old EB), respectively, before and 5 min. after isoproterenol perfusion.

(see details below) but was not arrhythmogenic, in CPVT cardiomyocytes isoproterenol caused the generation of after-contractions (which are the mechanical equivalent of DADs) and triggered activity. These arrhythmias were associated with elevation in the resting tension level (marked by the double-headed arrows in Fig. 6B and C), probably resulting from a prominent diastolic $[Ca^{2+}]_i$ rise as demonstrated in Figure 6F. Because in some of the CPVT preparations, pacing alone caused marked elevation in diastolic $[Ca^{2+}]_i$ followed by after-contractions and cessation of contractions, the response to isoproterenol was not tested in these experiments. Overall we performed 11 control experiments in none of which after-contractions or diastolic $[Ca^{2+}]_i$ rise were generated by isoproterenol. In the CPVT series we performed 15 experiments in two CPVT iPSCs clones. In five experiments (33%) pacing alone caused after-contractions in the absence of isoproterenol, in seven experiments (47%) isoproterenol generated after-contractions and triggered contractions, and in three experiments (20%) after-contractions were not generated either by pacing or isoproterenol.

An intriguing finding was that although isoproterenol induced arrhythmias in CPVT cardiomyocytes, it did not cause the common positive inotropic and lusitropic effects seen in control cardiomyocytes (Fig. 6A and D). As depicted by the representative control (Fig. 6A) and CPVT experiments (Fig. 6B and C) and the summary (Fig. 6D), whereas in control cardiomyocytes isoproterenol increased contraction amplitude (L_{Amp} +16.6% ± 2.9, $P < 0.05$; n = 5), the maximal rate of contraction and the maximal rate of relaxation ($dL/dt_{Contraction}$ + 23.8% ± 7.0, $P < 0.05$; $dL/dt_{Relaxation}$ + 33.5% ± 6.5, $P < 0.05$; n = 5), isoproterenol did not affect the contraction parameters of the CPVT cardiomyocytes (L_{Amp} –2.1% ± 4.2, $P > 0.05$; $dL/dt_{Contraction}$ +1.0% ± 9.5, $P > 0.05$; $dL/dt_{Relaxation}$ –0.4% ± 3.9, $P > 0.05$; n = 5). Concomitantly, in the CPVT cardiomyocytes (but not in control cardiomyocytes, Fig. 6E and F), isoproterenol caused a marked increase in diastolic $[Ca^{2+}]_i$; this key finding, which is a hallmark of the CASQ2 mutation, is likely to be responsible for the arrhythmias caused by the β-adrenergic stimulation.

Action potential characteristics in control and CPVT iPSCs-CMs

As the first step of the electrophysiological experiments, we characterized the basic action potential characteristics in control and iPSCs-CMs. To this end we obtained whole-cell current-clamp recordings from isolated dissociated spontaneously contracting areas. These representative recordings (Fig. 7A and B) demonstrated spontaneously generated action potentials with prominent pacemaker potential both in the control and the CPVT cardiomyocytes. Action potentials recordings from cardiomyocytes that beat spontaneously at a constant rate were analysed for action potential duration at 20% and 50% of repolarization (APD_{20}, APD_{50}), maximum diastolic potential (MDP), action potential amplitude (APA) and maximal rate of depolarization (dV/dt_{max}). In summary (Fig. 7), in CPVT cardiomyocytes APD_{20} (CPVT APD_{20} = 204.3 ± 24.7, Control APD_{20} = 124.1 ± 15.5, $P < 0.05$; n = 5) and APD_{50} (CPVT APD_{50} = 368.4 ± 41.4, Control APD_{50} = 201.01 ± 27.83, $P < 0.05$; n = 5) were longer than in control cardiomyocytes. Maximum diastolic potential, action potential amplitude and maximal rate of depolarization (dV/dt_{max}) were similar in both groups.

β-adrenergic stimulation causes delayed afterdepolarizations and oscillatory prepotentials in CPVT iPSCs-CMs

In vitro studies showed that under conditions of sympathetic activation, RyR2 and CASQ2 mutations are associated with SR diastolic Ca^{2+} leakage, leading to $[Ca^{2+}]_i$ overload. This in turn generates DADs, which can give rise to triggered activity underlying the clinical arrhythmias in CPVT patients [3]. In agreement with our expectations, in CPVT but not in control spontaneously contracting cardiomyocytes, exposure to isoproterenol generated DADs and oscillatory prepotentials. Specifically, although in control cardiomyocytes isoproterenol was non-arrhythmogenic (Fig. 8A), in CPVT cardiomyocytes isoproterenol caused prominent DADs, as demonstrated in two representative experiments (Fig. 8B and D, marked by red arrows). Importantly, in CPVT cardiomyocytes isoproterenol also caused oscillatory prepotentials, which are late diastolic depolarizations (Fig. 8C and D, marked by blue arrows). Altogether, whereas isoproterenol did not induce arrhythmias in any of the seven control experiments, DADs and/or oscillatory prepotentials were generated by isoproterenol in six out of the eight CPVT experiments (75%).

In summary, our results show that CPVT-derived cardiomyocytes are arrhythmic in response to β-adrenergic stimulation, and hence these novel findings demonstrate that cardiomyocytes generated from the CPVT patients' iPSCs display the clinical phenotype of catecholaminergic-mediated arrhythmias.

Discussion

In the present study we investigated the catecholamine-mediated arrhythmias in CASQ2-mutated cardiomyocytes, which were differentiated from iPSCs generated from CPVT patients. Our major findings were: (1) In CPVT iPSCs-CMs but not in control iPSCs-CMs, the β-adrenergic agonist isoproterenol caused marked elevation in diastolic $[Ca^{2+}]_i$, after-contractions, DADs and oscillatory prepotentials. (2) In contrast to control cardiomyocytes, in CPVT cardiomyocytes isoproterenol did not cause positive inotropic and lusitropic effects. (3) Ultrastructural analysis revealed that compared with control, CPVT cardiomyocytes displayed a more immature phenotype with unorganized myofilaments structure. Likewise, in CPVT cardiomyocytes, we observed extension of the SR cisternae and reduced number of caveolae.

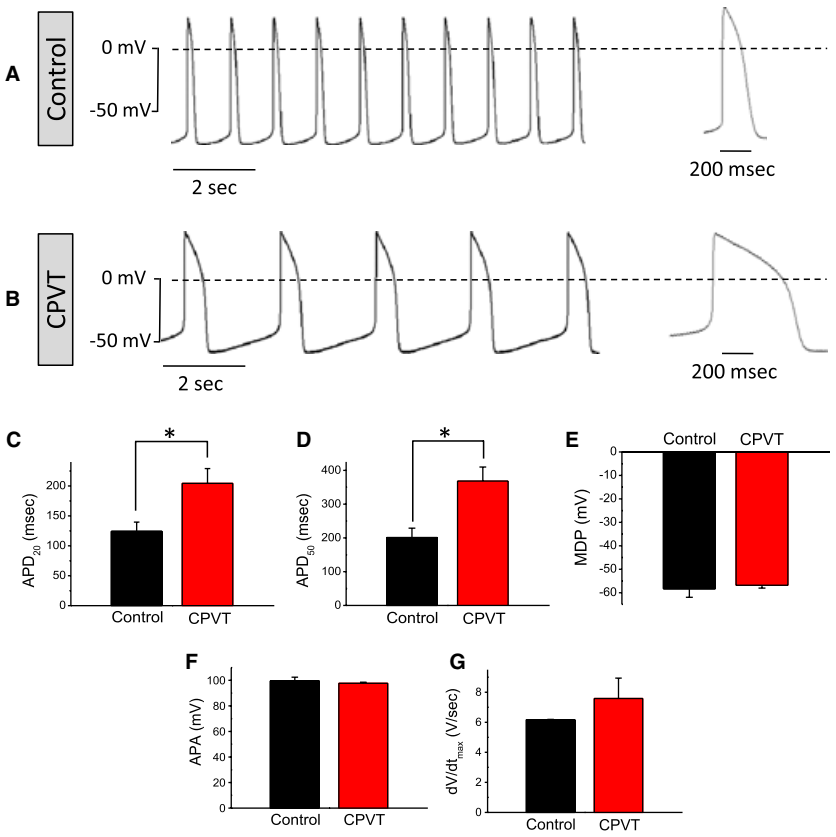

Fig. 7 Action potential characteristics of control and CPVT iPSCs-CMs. (**A**) Representative spontaneous action potentials recorded from control (**A**) and CPVT cardiomyocytes (**B**). A summary of action potential duration at 20% repolarization, APD_{20} (**C**), action potential duration at 50% repolarization, APD_{50} (**D**), maximum diastolic potential (MDP) (**E**), action potential amplitude (APA) (**F**), and maximal upstroke velocity of phase 0 depolarization, dV/dt_{max} (**G**), in control (black) and CPVT (red) cardiomyocytes. Note that in CPVT cardiomyocytes APD_{20} and APD_{50} were prolonged compared to control cells ($^*P < 0.05$).

CPVT iPSCs-CMs

Since the first generation of iPSCs a number of studies reported on the production of patient-specific iPSCs, which can be used as models of inherited human diseases. Recently several groups generated from patients with inherited cardiac disorders, iPSCs which were differentiated into functional cardiomyocytes [9–11]. To this end, in the present study we report for the first time on the generation of iPSCs from fibroblasts of two CPVT patients. Importantly, cardiomyocytes derived from these CPVT-derived iPSCs exhibited the key features of catecholaminergic-mediated arrhythmogenesis. The pluripotency of the reprogrammed cells was confirmed by their expression of typical pluripotent markers (Fig. 1C) and their capability to differentiate, through EBs and teratoma formation to all three germ layers (Fig. 1D and E). The presence of the missense mutation D307H in the CASQ2 gene was verified in both the parental patient's isolated fibroblasts and in the derived iPSCs (Fig. 2A and B). Thereafter, the cells were spontaneously differentiated into functional cardiomyocytes, as demonstrated by the expression of the cardiac myofilaments proteins (α-sarcomeric actinin and troponin I) organized in sarcomeric structures (Fig. 3A). PCR analysis of control and CPVT iPSCs and hESCs H9.2 EBs (Fig. 3B) showed the mRNA expression of CASQ2, calreticulin, junctin, triadin, NCX1, SERCA2 and RyR2, which are involved in intracellular Ca^{2+} handling. No apparent difference was observed in the expression of these genes between the control and CPVT iPSCs-EBs. Cardiomyocytes derived from both control and CPVT iPSCs similarly expressed the cardiac calsequestrin protein (demonstrated by the immunofluorescence staining, Fig. 4), although cardiomyocytes derived from hESCs H9.2 did not express the protein, as was previously reported [16, 19, 20]. In the present study, similar to previous immunofluorescence staining findings in cardiomyocytes generated from ESCs (recombinant CASQ2) [20] and iPSCs [17], we found that the staining pattern of CASQ2 is different from adult mouse ventricular myocytes [5, 6] in which CASQ2 is co-localized with the Z bands. This dissimilarity with adult cardiomyocytes probably results from the immaturity of cardiomyocytes generated from ESCs or iPSCs, which among other differences present poorly developed SR that is more sparse in the cytoplasm compared to adult cardiomyocytes, as seen by the TEM analysis. Finally, the mean spontaneous beating rate of CPVT iPSCs-CMs was slower than control iPSCs-CMs by

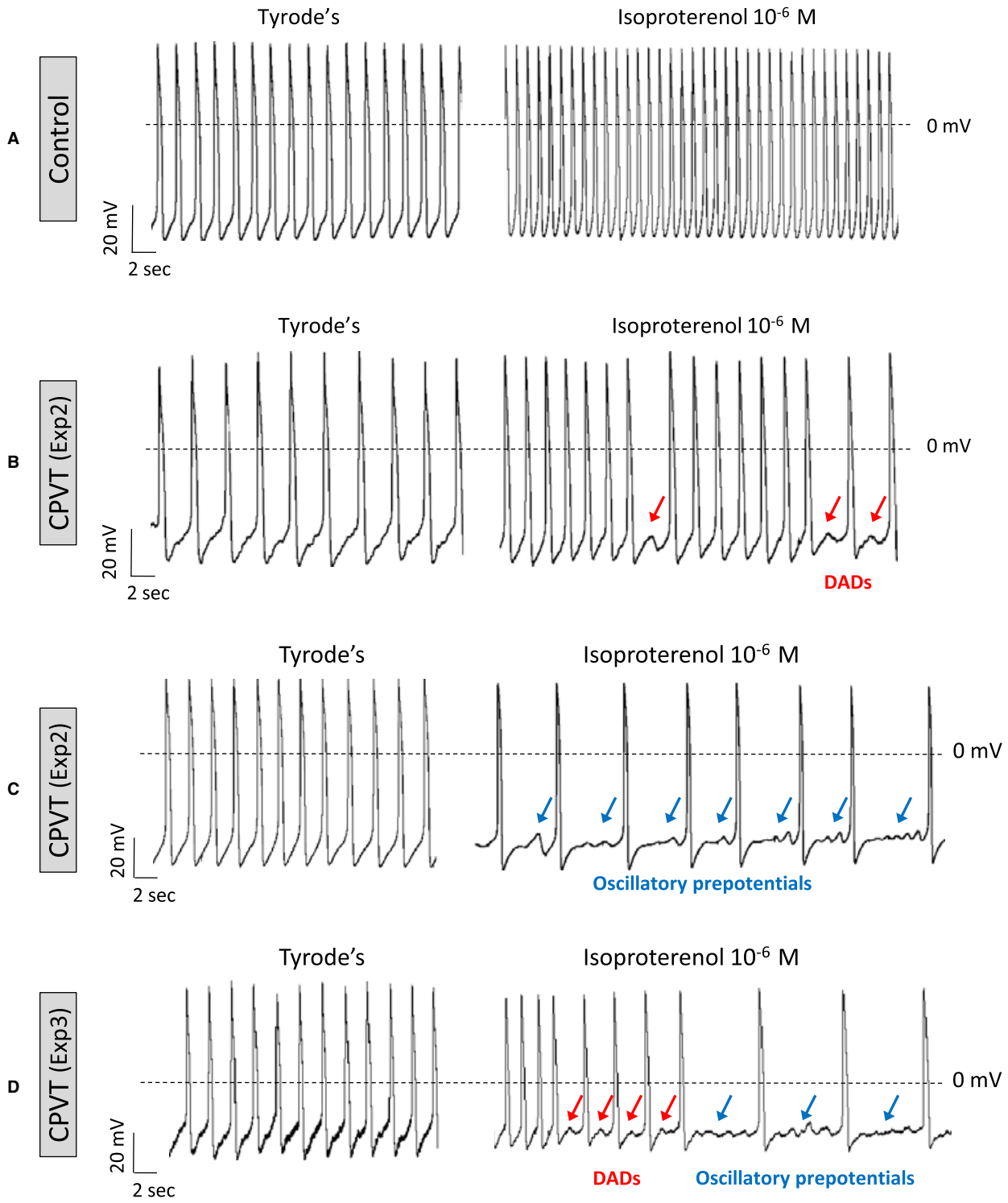

Fig. 8 Isoproterenol caused DADs and oscillatory prepotentials in CPVT iPSCs-CMs. (**A**) Representative spontaneous recordings from control cardiomyocytes (30-day-old EB), and (**B**–**D**) CPVT cardiomyocytes (32-, 30- and 32-day-old EBs, respectively) in the absence (Tyrode's) and presence of isoproterenol. Note that only in CPVT cardiomyocytes, isoproterenol caused DADs (red arrows) or oscillatory prepotentials (blue arrows).

~34%. These findings, which still need to be established in a larger number of preparations and different clones, are in agreement with studies reporting a lower resting heart rate among CPVT patients [21, 22].

Ultrastructural changes in CPVT iPSCs-CMs

Ultrastructural assessment of CPVT cardiomyocytes showed small expansion of the SR cisternae, as previously reported in a mouse model of CPVT with a deficient cardiac calsequestrin [5, 23, 24]. This expansion was suggested to constitute a compensatory response for the loss of SR Ca^{2+} buffering by the mutated CASQ2 [24]. As previously reported in cardiomyocytes derived from ESCs and iPSCs [18, 25], T-tubules were not observed in control and CPVT iPSCs-CMs, which is explained by the findings that T tubules formation occurs relatively late in mammalian cardiomyocytes development. The ultrastructural analysis also demonstrated that compared with control, CPVT cardiomyocytes have fewer caveolae [24], which participate in a variety of cellular functions such as signal transduction and Ca^{2+} homeostasis [26–28]. A number of different ion channels and transporters have been localized to caveolae in cardiac myocytes, including the L-type Ca^{2+} channel (Cav1.2), Na^{+} channels (Nav1.5), pacemaker channels (HCN4) and the Na^{+}/Ca^{2+} exchanger (NCX1) [26]. The observations showing that excitation-contraction coupling and β-adrenergic signalling molecules are concentrated in the caveolae (suggesting the caveolae play an important role in these signalling pathways [27]) and a connection between caveolae disruption and arrhythmias [26], imply that the reduced number of caveolae in CPVT iPSCs-CMs may contribute to this disease-specific arrhythmias [26].

Arrhythmias in CPVT iPSCs-CMs

The fundamental features of isoproterenol-induced arrhythmias presented by CPVT cardiomyocytes exemplified by the electrophysiological and mechanical recordings (Figs 6 and 8) suggest that these mutated cardiomyocytes constitute a reliable model for investigating the arrhythmias occurring in CPVT patients. We report here for the first time that in addition to the familiar DADs occurring in $CPVT^{D307H}$ mutant cardiomyocytes in response to β-adrenergic stimulation [1, 3, 5], isoproterenol also caused arrhythmogenic depolarizing oscillatory prepotentials, which were originally described in cardiac muscle by Bozler in 1942 [29, 30]. In contrast to DADs that follow the action potential and therefore appear during the *early* diastolic depolarization, oscillatory prepotentials are defined as diastolic voltage oscillations, which appear during the *late* diastolic depolarization [31, 32]. The oscillatory prepotentials have a longer duration than DADs, they overshoot and undershoot the late diastolic depolarization, and grow progressively in amplitude until reaching the threshold and initiating spontaneous activity [31, 32]. As clearly seen in the representative experiments, CPVT cardiomyocytes exposed to isoproterenol developed DADs (Fig. 8B) and the corresponding after-contractions (Fig. 6), oscillatory prepotentials (Fig. 8C) or both (Fig. 8D). DADs defined as voltage oscillations which follow an action potential and occur at the beginning of the diastolic depolarization, may cause cessation of the next spontaneous action potential [32, 33]. Indeed, in Figure 8B and D we show in spontaneously active CPVT cardiomyocytes exposed to isoproterenol, prominent DADs which in some cases suppressed the generation of the spontaneous action potentials.

An important finding in CPVT cardiomyocytes was that β-adrenergic stimulation caused marked diastolic $[Ca^{2+}]_i$ rise (Fig. 6F), which is a principal feature of the CASQ2 mutation. This key phenomenon is consistent with a similar increase in diastolic $[Ca^{2+}]_i$ demonstrated in paced cardiomyocytes from mutant mouse with deficient $CASQ2^{307/307}$, in the presence of isoproterenol [7]. Hence, the diastolic $[Ca^{2+}]_i$ rise is likely to be the prime initiator of both the DADs and oscillatory prepotentials, which can be induced by high $[Ca^{2+}]_o$ and β-adrenergic stimulation, and thus depend on increased $[Ca^{2+}]_i$ [31, 32]. Finally, although isoproterenol generated arrhythmias in CPVT cardiomyocytes (but not in control cardiomyocytes), the commonly seen positive inotropic and lusitropic effects were not observed (Fig. 6). The mechanism underlying this behaviour was not investigated in the present study.

The implication of generating iPSCs-CMs from patients with inherited cardiac diseases

CPVT is a complex disease which poses several challenges in the management of affected patients [34]. Because despite the recent advancement in understanding the diverse aspects of CPVT this fatal disease still presents high mortality rates among young and older individuals, there is an emerging need for developing targeted pharmacological agents. Thus far only few groups have studied the pathogenesis of the autosomal recessive variant of CPVT, exploiting $CASQ2^{D307H}$ mutation in rat or mouse models, and demonstrated that disturbed Ca^{2+} handling and complex ventricular arrhythmias are similar to the CPVT phenotype observed in human patients [3]. Nevertheless, as recently stated by Priori's group [34], 'the chance of discovering new strategies to treat CPVT is tightly dependent upon the progress in understanding the molecular and the electrophysiological determinants of the CPVT phenotype and of the relationships between intracellular Ca^{2+} regulation and arrhythmogenesis'. Patient-specific iPSCs can provide useful platforms for the discovery of unprecedented insights into disease mechanisms, as well as new drugs [35]. Indeed, since the seminal breakthrough of generating iPSCs [36, 37], several patient-specific iPSCs lines were developed for a variety of diseases, including neurodegenerative diseases and metabolic disorders [38, 39]. In this regard, Moretti *et al.* [9], Itzhaki *et al.* [10] and Yazawa *et al.* [11] recently generated iPSCs from patients with inherited cardiac diseases, and demonstrated that their derived cardiomyocytes exhibit the electrophysiological features of the disorder, thus supporting the suitability of iPSCs-derived

cardiomyocytes to serve as a platform for exploring disease mechanisms in human genetic cardiac disorders. Hence, the derivation of cardiomyocytes from CPVT patients' iPSCs can provide the means to study in the mutated myocytes, the functional changes and the underlying molecular mechanisms of CASQ2-related CPVT, and therefore advance our understanding of CPVT and consequently improve its future clinical outcome.

From a mechanistic point of view it was important to discover that the arrhythmogenic substrate of CPVT are DADs and oscillatory prepotentials, which probably develop as a consequence of the mutation-related diastolic $[Ca^{2+}]_i$ elevation. Although DADs were described *in vitro* and *in vivo,* the demonstration that they were responsible for arrhythmogenesis in humans was largely a consequence of genetic research [40]. Therefore, our findings demonstrating the generation of DADs as well as oscillatory prepotentials in CPVT patients-derived cardiomyocytes are of prime importance.

In summary, we derived CPVT iPSCs, which gave rise to functional cardiomyocytes exhibiting the disease-specific arrhythmogenic characteristics. These accomplishments demonstrate our ability to generate an experimental system, which can exhibit the features of human genetic cardiac disorders, such as CPVT, in which the disease mechanisms can be explored and candidate drugs can be screened and developed in the physiologic and disease-causing settings on a patient-specific level.

Acknowledgements

We wish to thank Irina Reiter, Igal Germanguz, Sivan Eliyahu and Anna Ziskind for their technical assistance, and Ilana Laevsky and Dr. Tzipora Falik-Zaccai for the karyotype analysis. We wish to express our deepest appreciation and gratitude to Dr. Mihaela Gherghiceanu for her professional and excellent TEM analysis.

Funding source: This work was supported by the Ministry of Science and Technology (MOST), Israel Science Foundation (ISF), Ministry of Health – Chief Scientist, the Rappaport Family Institute for Research in the Medical Sciences and The Sohnis and Forman Families Stem Cells Center.

References

1. **Priori SG, Napolitano C, Tiso N, *et al.*** Mutations in the cardiac ryanodine receptor gene (hRyR2) underlie catecholaminergic polymorphic ventricular tachycardia. *Circulation* 2001; 103: 196–200.
2. **Lahat H, Pras E, Olender T, *et al.*** A missense mutation in a highly conserved region of CASQ2 is associated with autosomal recessive catecholamine-induced polymorphic ventricular tachycardia in Bedouin families from Israel. *Am J Hum Genet*. 2001; 69: 1378–84.
3. **Viatchenko-Karpinski S, Terentyev D, Gyorke I, *et al.*** Abnormal calcium signaling and sudden cardiac death associated with mutation of calsequestrin. *Circ Res*. 2004; 94: 471–7.
4. **di Barletta MR, Viatchenko-Karpinski S, Nori A, *et al.*** Clinical phenotype and functional characterization of CASQ2 mutations associated with catecholaminergic polymorphic ventricular tachycardia. *Circulation*. 2006; 114: 1012–9.
5. **Dirksen WP, Lacombe VA, Chi M, *et al.*** A mutation in calsequestrin, $CASQ2^{D307H}$, impairs Sarcoplasmic Reticulum Ca^{2+} handling and causes complex ventricular arrhythmias in mice. *Cardiovasc Res*. 2007; 75: 69–78.
6. **Kalyanasundaram A, Bal NC, Franzini-Armstrong C, *et al.*** The calsequestrin mutation $CASQ2^{D307H}$ does not affect protein stability and targeting to the junctional sarcoplasmic reticulum but compromises its dynamic regulation of calcium buffering. *J Biol Chem*. 2009; 285: 3076–83.
7. **Song L, Alcalai R, Arad M, *et al.*** Calsequestrin 2 (CASQ2) mutations increase expression of calreticulin and ryanodine receptors, causing catecholaminergic polymorphic ventricular tachycardia. *J Clin Invest*. 2007; 117: 1814–23.
8. **Terentyev D, Nori A, Santoro M, *et al.*** Abnormal interactions of calsequestrin with the ryanodine receptor calcium release channel complex linked to exercise-induced sudden cardiac death. *Circ Res*. 2006; 98: 1151–8.
9. **Moretti A, Bellin M, Welling A, *et al.*** Patient-specific induced pluripotent stem-cell models for long-QT syndrome. *N Engl J Med*. 2010; 363: 1397–409.
10. **Itzhaki I, Maizels L, Huber I, *et al.*** Modelling the long QT syndrome with induced pluripotent stem cells. *Nature*. 2011; 471: 225–9.
11. **Yazawa M, Hsueh B, Jia X, *et al.*** Using induced pluripotent stem cells to investigate cardiac phenotypes in Timothy syndrome. *Nature*. 2011; 471: 230–4.
12. **Novak A, Shtrichman R, Germanguz I, *et al.*** Enhanced reprogramming and cardiac differentiation of human keratinocytes derived from plucked hair follicles, using a single excisable lentivirus. *Cell Reprogram*. 2010; 12: 665–78.
13. **Somers A, Jean JC, Sommer CA, *et al.*** Generation of transgene-free lung disease-specific human iPS cells using a single excisable lentiviral stem cell cassette. *Stem Cells*. 2010; 28: 1728–40.
14. **Sommer CA, Stadtfeld M, Murphy GJ, *et al.*** Induced pluripotent stem cell generation using a single lentiviral stem cell cassette. *Stem Cells*. 2009; 27: 543–9.
15. **Sedan O, Dolnikov K, Zeevi-Levin N, *et al.*** 1,4,5-Inositol trisphosphate-operated intracellular $Ca(^{2+})$ stores and angiotensin-II/endothelin-1 signaling pathway are functional in human embryonic stem cell-derived cardiomyocytes. *Stem Cells*. 2008; 26: 3130–8.
16. **Dolnikov K, Shilkrut M, Zeevi-Levin N, *et al.*** Functional properties of human embryonic stem cell-derived cardiomyocytes: intracellular Ca^{2+} handling and the role of sarcoplasmic reticulum in the contraction. *Stem Cells*. 2006; 24: 236–45.
17. **Germanguz I, Sedan O, Zeevi-Levin N, *et al.*** Molecular characterization and functional properties of cardiomyocytes derived from human inducible pluripotent stem cells. *J Cell Mol Med*. 2009; 15: 38–51.

18. **Gherghiceanu M, Barad L, Novak A, *et al.*** Cardiomyocytes derived from human embryonic and induced pluripotent stem cells: comparative ultrastructure. *J Cell Mol Med*. 2011; 15: 2539–51.
19. **Liu J, Fu JD, Siu CW, *et al.*** Functional sarcoplasmic reticulum for calcium handling of human embryonic stem cell-derived cardiomyocytes: insights for driven maturation. *Stem Cells*. 2007; 25: 3038–44.
20. **Liu J, Lieu DK, Siu CW, *et al.*** Facilitated maturation of Ca^{2+} handling properties of human embryonic stem cell-derived cardiomyocytes by calsequestrin expression. *Am J Physiol Cell Physiol*. 2009; 297: C152–9.
21. **Katz G, Arad M, Eldar M**. Catecholaminergic polymorphic ventricular tachycardia from bedside to bench and beyond. *Curr Probl Cardiol*. 2009; 34: 9–43.
22. **Postma AV, Denjoy I, Kamblock J, *et al.*** Catecholaminergic polymorphic ventricular tachycardia: RYR2 mutations, bradycardia, and follow up of the patients. *J Med Genet*. 2005; 42: 863–70.
23. **Rizzi N, Liu N, Napolitano C, *et al.*** Unexpected structural and functional consequences of the R33Q homozygous mutation in cardiac calsequestrin: a complex arrhythmogenic cascade in a knock in mouse model. *Circ Res*. 2008; 103: 298–306.
24. **Knollmann BC, Chopra N, Hlaing T, *et al.*** Casq2 deletion causes sarcoplasmic reticulum volume increase, premature Ca^{2+} release, and catecholaminergic polymorphic ventricular tachycardia. *J Clin Invest*. 2006; 116: 2510–20.
25. **Di Maio A, Karko K, Snopko RM, *et al.*** T-tubule formation in cardiacmyocytes: two possible mechanisms? *J Muscle Res Cell Motil*. 2007; 28: 231–41.
26. **Balijepalli RC, Kamp TJ**. Caveolae, ion channels and cardiac arrhythmias. *Prog Biophys Mol Biol*. 2008; 98: 149–60.
27. **Calaghan S, White E**. Caveolae modulate excitation-contraction coupling and beta2-adrenergic signalling in adult rat ventricular myocytes. *Cardiovasc Res*. 2006; 69: 816–24.
28. **Patel HH, Murray F, Insel PA**. Caveolae as organizers of pharmacologically relevant signal transduction molecules. *Annu Rev Pharmacol Toxicol*. 2008; 48: 359–91.
29. **Bozler E**. The initiation of impulses in cardiac muscle. *Am J Physiol*. 1942; 138: 273–82.
30. **Cranefield PF**. Action potentials, afterpotentials, and arrhythmias. *Circ Res*. 1977; 41: 415–23.
31. **Catanzaro JN, Nett MP, Rota M, *et al.*** On the mechanisms underlying diastolic voltage oscillations in the sinoatrial node. *J Electrocardiol*. 2006; 39: 342.
32. **Kim EM, Choy Y, Vassalle M**. Mechanisms of suppression and initiation of pacemaker activity in guinea-pig sinoatrial node superfused in high [K+]o. *J Mol Cell Cardiol*. 1997; 29: 1433–45.
33. **Rosen MR, Moak JP, Damiano B**. The clinical relevance of afterdepolarizations. *Ann N Y Acad Sci*. 1984; 427: 84–93.
34. **Mohamed U, Napolitano C, Priori SG**. Molecular and electrophysiological bases of catecholaminergic polymorphic ventricular tachycardia. *J Cardiovasc Electrophysiol*. 2007; 18: 791–7.
35. **Kiskinis E, Eggan K**. Progress toward the clinical application of patient-specific pluripotent stem cells. *J Clin Invest*. 2010; 120: 51–9.
36. **Takahashi K, Tanabe K, Ohnuki M, *et al.*** Induction of pluripotent stem cells from adult human fibroblasts by defined factors. *Cell*. 2007; 131: 861–72.
37. **Yu J, Vodyanik MA, Smuga-Otto K, *et al.*** Induced pluripotent stem cell lines derived from human somatic cells. *Science*. 2007; 318: 1917–20.
38. **Maehr R, Chen S, Snitow M, *et al.*** Generation of pluripotent stem cells from patients with type 1 diabetes. *Proc Natl Acad Sci USA*. 2009; 106: 15768–73.
39. **Soldner F, Hockemeyer D, Beard C, *et al.*** Parkinson's disease patient-derived induced pluripotent stem cells free of viral reprogramming factors. *Cell*. 2009; 136: 964–77.
40. **Priori SG**. The fifteen years of discoveries that shaped molecular electrophysiology: time for appraisal. *Circ Res*. 2010; 107: 451–6.